Multiblock Copolymers Based on Highly Crystalline Polyethylene and Soft Poly(ethylene-co-butadiene) Segments: Towards Polyolefin Thermoplastic Elastomers

Marvin Langlais, Nicolas Baulu, Séverin Dronet, Charlotte Dire, François Jean-Baptiste-Dit-Dominique, David Albertini, Franck D'Agosto, Damien Montarnal, Christophe Boisson

Multiblock copolymers based on highly crystalline polyethylene and soft poly(ethylene-*co*-butadiene) segments: towards polyolefin thermoplastic elastomers.

Marvin Langlais,[a] Nicolas Baulu,[a,b] Séverin Dronet,[b] Charlotte Dire,[b] François Jean-Baptiste-dit-Dominique,[b] David Albertini,[c] Franck D'Agosto,*[a] Damien Montarnal,*[a] and Christophe Boisson*[a]

[a] Dr. M. Langlais, Dr. N. Baulu, Dr. F. D'Agosto, Dr. D. Montarnal, Dr. C. Boisson
Université Claude Bernard Lyon 1, CPE Lyon, CNRS UMR 5128, Laboratoire CP2M, Equipe PCM, 69616 Villeurbanne, France
E-mail: christophe.boisson@univ-lyon1.fr, damien.montarnal@univ-lyon1.fr, franck.dagosto@univ-lyon1.fr

[b] Dr. N. Baulu, Dr. S. Dronet, Dr. C. Dire, Dr. F. Jean-Baptiste-dit-Dominique
Manufacture Michelin, 23 place Carmes Déchaux, F-63000 Clermont-Ferrand, France

[c] Dr. D. Albertini
Université Claude Bernard Lyon 1, INSA Lyon, CNRS UMR 5270, Institut des Nanotechnologies de Lyon, 69616 Villeurbanne, France

Supporting information for this article is given via a link at the end of the document

Abstract: Block copolymers based on polyethylene (PE) and ethylene butadiene rubber (EBR) were obtained by successive controlled coordinative chain transfer polymerization (CCTP) of a mixture of ethylene and butadiene (80/20) and pure ethylene. EBR-*b*-PE diblock copolymers were synthesized using $\{Me_2Si(C_{13}H_8)_2Nd(BH_4)_2Li(THF)\}_2$ complex in combination with *n*-butyl,*n*-octyl magnesium (BOMAG) used as both alkylating and chain transfer agent (CTA). Triblock and multiblock copolymers featuring highly semi-crystalline PE hard segments and soft EBR segments were further obtained via the development of a bimetallic CTA, the pentanediyl-1,5-di(magnesium bromide) (PDMB). These new block copolymers undergo crystallization-driven organization into lamellar structures and exhibit a variety of mechanical properties, including excellent extensibility and elastic recovery in the case of triblock and multiblock copolymers.

Introduction

The properties of thermoplastic elastomers (TPE) are strongly dependent on the structuration at the micro- or nanoscale between a major elastomeric phase and a minor rigid phase playing the role of physical cross-links. Either obtained through reactive processing or self-organization, these materials are not based on chemical cross-linking percolating through the continuous phase which allows them to be (re)transformed like thermoplastics and recycled. This class of materials is thus particularly appealing in the context of circular economy. Consequently, it appears necessary to develop new classes of TPEs to improve their overall environmental impact and broaden their range of usage properties. This can be achieved by controlling the glass transition temperature (T_g) of the soft matrix and increasing the T_g or the melting temperature (T_m) of the rigid domains.[1] A number of TPEs have been developed industrially from the step-growth polymerization of a large variety of building blocks such as polyurethanes, polyether block amides, polyether block esters.[2] Well-controlled or living chain growth strategies able the control precisely the macromolecular architecture of block copolymers with soft and rigid segments offer however easier handles to fine-tune the morphologies of the materials, that directly impacts their thermomechanical properties. As an example, block copolymers obtained by living anionic polymerization such as polystyrene-*b*-polybutadiene-*b*-polystyrene (PS-*b*-PB-*b*-PS also called SBS) and polystyrene-*b*-polyisoprene-*b*-polystyrene (PS-*b*-PI-*b*-PS, SIS) are ubiquitous class of TPEs.[1] Recent developments can be highlighted in the domain of polyesters such as switchable catalysis[3],[4] or chain-shuttling copolymerization[5] that paves the way to sequence-defined architectures.

Polyolefin thermoplastic elastomers (P-TPEs) constitute another attractive class of materials for their high performance and economical sourcing. Different synthesis strategies from coordination polymerization and challenges in this field have been thoroughly discussed in this area in a recent review.[6] A large range of amorphous or crystalline polyolefins can be obtained by (co)polymerizing a very narrow set of easily available and cheap monomers such as ethylene (E), α-olefins or conjugated dienes. These materials also combine several highly valuable properties such as high entanglement moduli (above 1 MPa) and low T_g. The living polymerization by coordination-insertion polymerization of olefins (E, propene (P), α-olefins) has also been extensively studied to produce block copolymers with remarkable properties.[7] However, only one polymer chain is produced per metallic active center, which considerably increases the overall cost and the amount metallic residues, and thus reduces the possibility of large-scale production of these polymers. Coordinative chain transfer polymerization (CCTP) allows generating a very large number of polymeric chains per metallic active center. This controlled coordination-insertion polymerization technique takes advantage of degenerative chain-transfer between the metallic active center used as a catalyst and an organometallic chain transfer agent (CTA) such as MgR_2, ZnR_2 or AlR_3.[8–12] Diblock and multiblock copolymers have been synthesized via CCTP. At Dow Chemical researchers obtained multiblock copolymers,[13,14] now commercialized by the tradename INFUSE™, by combining two catalysts with a common CTA, $ZnEt_2$, in the presence of E and octene (Oct). Oct being preferentially copolymerized with E by one of the two catalysts, soft P(E-*co*-Oct) and rigid PE segments are formed within the same chains. More recently, using a single catalyst, Lee and coll. successfully prepared by CCTP PE-*b*-P(E-*co*-P)-*b*-PE triblock copolymers by successive polymerization of E and a mixture of E and P followed by a coupling reaction.[15] The same group has developed a divalent chain transfer agent based on zinc.[16] PS-*b*-P(E-*co*-P)-*b*-PS triblock copolymers have been obtained by

successive pyridyl-amido hafnium catalyst-mediated coordination-insertion copolymerization of E and P and anionic polymerization of styrene.

We showed that a new class of elastomers can be formed by copolymerizing E and butadiene (B) with the catalysts $\{Me_2Si(C_{13}H_8)_2Nd(BH_4)_2Li(THF)\}_2/MgR_2$.[17],[18] Called ethylene butadiene rubbers (EBR), these elastomers feature ethylene units, *trans*-1,4- and vinyl butadiene units and cyclohexyl motifs formed by intramolecular cyclisation (Scheme 1). More recently, we have highlighted that this catalyst fulfills the requirement of CCTP[19] and is amenable to the design of macromolecular architectures incorporating EBR segments.[20],[21]

Satisfactory elastomeric properties include low moduli, high extensibility and high elastic recovery after deformation.[22] In the case of TPEs from block copolymers, such properties are strongly linked with the proper separation of hard segments into non-continuous domains, and proper anchoring of the soft segments across hard domains thanks to triblock or multiblock architectures. Widely used SBS- or SIS-type TPEs feature high incompatibility between the PS and PB or PI segments, which ensures strong segregation in the melt and easy control of the morphology by tuning the volumic fraction of PS. Polyolefin block copolymers feature low incompatibility in the melt, and often rely on crystallization-induced phase separation from weakly segregated melts.[23] They display in this way an advantageous combination of good mechanical performances and low melt viscosities.

The present paper demonstrates that well-defined diblock, triblock and multiblock copolymers featuring soft EBR and crystalline PE segments can be prepared using $\{Me_2Si(C_{13}H_8)_2Nd(BH_4)_2Li(THF)\}_2$ (**1**)/MgR_2 as a catalyst according to CCTP. Structural, mechanical and rheological characterization confirms that although these materials are made from more than 80 wt% E overall, the phase separation between the crystalline PE domains and the soft EBR phase leads to remarkable performances as TPEs.

Results and Discussion

Synthesis of diblock copolymers via CCTP

As mentioned in the introduction, the copolymerization of ethylene with butadiene using $\{Me_2Si(C_{13}H_8)_2Nd(BH_4)_2Li(THF)\}_2$ (**1**)/(*n*-Bu)(*n*-Oct)Mg (BOMAG) catalyst is controlled by a mechanism of CCTP and thus well-adapted to the design of block copolymers.

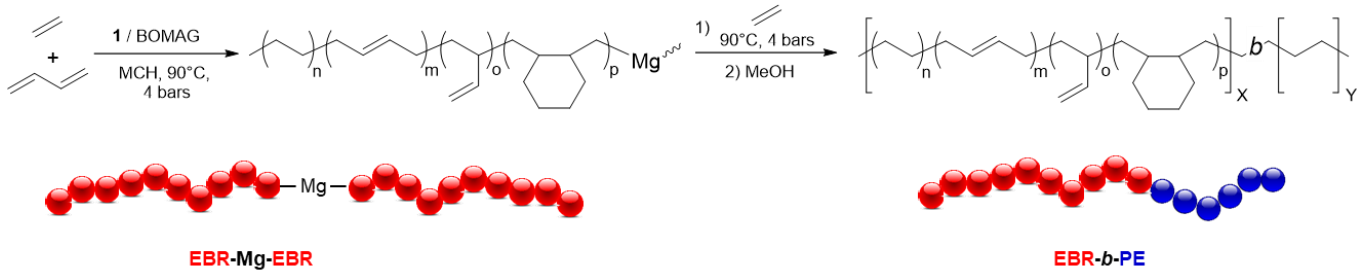

Scheme 1. Synthesis of EBR-*b*-PE diblock copolymers via CCTP.

First, diblock copolymers EBR-*b*-PE (Scheme 1 and Table 1, runs 2,4-6,8) were prepared in a single reactor by changing the feed from an ethylene-butadiene mixture to pure ethylene. The theoretical molar mass of each block is directly monitored by the consumption of monomers during each step (i.e. pressure decay in the ballast), the number of chains being fixed by the amount of BOMAG. Reference EBRs were prepared as models for EBR segments before chain extension (Table 1, runs 1, 3, 7). As already reported, a good control of the copolymerization was confirmed by the good match between theoretical and measured molar masses and rather low dispersity values. For each diblock copolymers (runs 2, 4-6, 8 in Table 1), there is also a good agreement between the theoretical and experimental M_n, although a broadening of the molar mass distribution is observed for the highest PE molar mass targeted (runs 6 and 8 in Table 1). Such broadening could be due to β-H elimination during the second step leading to dead EBR-*b*-PE chains and PE chains after reinitiation. However, PE could not be detected by SEC (Figure S2 and S3) although its formation cannot be completely ruled out. We believe that the broadening could indeed originate from the variety of chain ends of the EBR block, such as alkyl, cyclohexyl-methylene or (vinylcyclohexyl)-methylene depending on the different insertion modes of butadiene and reinsertion of pendant double bonds.[19] Without impeding the formation of block copolymers after chain extension, the corresponding various reactivities towards ethylene insertion during chain extension would broaden the final molar mass distribution. We indeed previously highlighted that the catalytic insertion of ethylene after (vinylcyclohexyl)-methylene terminal groups is significantly slower than after other terminal groups. On the other hand, for polymers with higher molar masses, the viscosity of the polymerization medium increases significantly during the course of polymerization. This may affect chain transfer rates and increase the dispersity values.

Diblock copolymers of increasing molar masses (Table 1, runs 2, 5, 8) were synthesized keeping the same fraction of PE (~17 wt%). SEC analyses of the reference EBRs and of the corresponding diblock copolymers showed successful chain extensions (Figure S2). In addition, the three diblock copolymers displayed very similar microstructures as expected (Table S1). A series of diblock copolymers based on a EBR with a targeted M_n of 30 kg mol^{-1} (EBR_{30K}) with an increasing fraction of PE were also prepared (runs 4-6 in Table 1). As expected, the percentage of ethylene units increases from an EBR to an EBR-*b*-PE block copolymers (Table S2).

Table 1. Molar masses and thermal properties of EBR and EBR-*b*-PE diblock copolymers discussed in this manuscript.

Run	Polymer	[BOMAG] (mmol L^{-1})	Yield (g)	M_n theo [a] (g mol^{-1})	M_n SEC [b] (g mol^{-1})	$Đ$ [b]	T_g [c] (°C)	T_m [c] (°C)	T_c [c] (°C)	PE fraction (wt %)	Crystallinity of PE segments[d] (%)
1	EBR_{15K}	2.5	15.8	15800	13300	1.3	-33.4	-	-	-	-
2	EBR_{15K}-*b*-PE_{3K}	2.5	18.9	18900	17100	2.2	-32.9	105.2	80.1	17	15
3	EBR_{30K}	1.25	14.7	29400	28700	1.4	-33.2	-	-	-	-
4	EBR_{30K}-*b*-PE_{3K}	1.25	17.2	34400	33700	1.7	-33.2	105.3	80.1	9	33
5	EBR_{30K}-*b*-PE_{6K}	1.25	18.4	36800	38200	2.2	-32.7	118.6	107.4	17	49
6	EBR_{30K}-*b*-PE_{12K}	1.25	21.1	42200	41000	2.7	-32.5	124.6	111.0	29	55
7	EBR_{45K}	0.82	15.5	47200	47600	1.8	-33.1	-	-	-	-
8	EBR_{45K}-*b*-PE_{9K}	0.82	18.5	56400	43200	2.5	-32.5	116.5	97.4	17	41

XK stands for X*1000 g $mol^{-1}$and designates the targeted number-average molar mass (see calculation hereafter) of the considered chain. Conditions: 200 mL of methylcyclohexane (MCH), 4 bars, 90°C, E/B = 80/20 mol%, [Nd] = 250 µM. [a] M_n^{theo} = yield/(n_{CTA} x 2). [b] Determined by SEC in THF at 35°C for EBR and in 1,2,4-trichlorobenzene at 150°C for diblock copolymers. [c] Determined by DSC. [d] Determined by DSC ($\Delta H_{100\%PE}$ = 293 J g^{-1}) and normalized to the PE weight fraction.

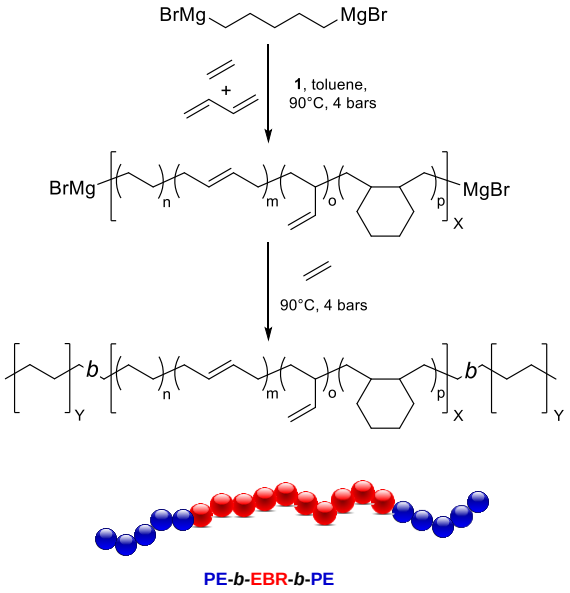

Scheme 2. Synthesis of triblock copolymers using a (**1**)/PDMB catalyst.

Bimetallic CTA for the synthesis of EBR and triblock copolymers

The preparation of triblock copolymers PE-*b*-EBR-*b*-PE is more challenging. It requires either the implementation of a very efficient coupling reaction when the diblock copolymers are formed or the design of a divalent (bimetallic) CTA such as magnesium complexes of formula $XMg(CH_2)_nMgX$. In a previous work, we have synthesized and implemented in polymerization of olefins the pentanediyl-1,5-di(mesitylmagnesium) CTA ($MesMg(CH_2)_5MgMes$). In association with the complex **1**, a selective polymer chain growth on the pentanediyl moiety was demonstrated, the mesityl moiety remaining unreactive.[24]

During the course of this work, we realized that the ability of Grignard reagents such as butylmagnesium bromide (BMB) to act both as alkylating agent and CTA was specific to the use of complex **1** (Table S3). Indeed BMB does not activate bis-pentamethylcyclopentadienyl neodymium precursors such as $(C_5Me_5)_2NdCl_2Li(OEt_2)_2$ and $((C_5Me_5)_2Nd(BH_4)(THF)$ for ethylene polymerization. The pentanediyl-1,5-di(magnesium bromide) ($BrMg(CH_2)_5MgBr$ - PDMB) was then anticipated to be an efficient CTA when used in combination with **1** for the synthesis of the targeted PE-*b*-EBR-*b*-PE triblock copolymers (Scheme 2). PDMB was prepared by reacting dibromopentane with magnesium in 2-methyltetrahydrofuran (MeTHF). After evaporation of the solvent, the product was solubilized in toluene (0.43 M, MeTHF/Mg = 2.15). The control of the copolymerization of E and B by the **1**/PDMB catalyst was first demonstrated when forming EBR using various amounts of PDMB. As expected, a decrease of M_n was observed when increasing the concentration of the CTA (runs S3-S6 in Table S3) while dispersity values as low as 1.4 could be obtained, similarly to dispersities previously obtained with **1**/BOMAG. PDMB was next implemented to synthesize triblock copolymers by achieving EBR by sequential copolymerization of E with B followed by its chain extension in the presence of E (Scheme 2) in a one-pot process. Two triblock copolymers with overall 17 wt% PE were prepared from EBR blocks of M_n of *ca* 30 and 60 kg mol^{-1} (Table 2, runs 9 and 10, respectively) according to the same previously described procedure employed for the synthesis of the EBR-*b*-PE diblock copolymers with BOMAG. SEC traces of the isolated triblock copolymers (Figure S4) were

unimodal showing the formation of the desired triblock copolymers.

The control of the monomer feeds and the pseudo-living nature of the polymerization enable multiple switches from a mixture of E and B to pure E while forming multiblock copolymers with PE and EBR segments. This was indeed achieved up to an heptablock copolymer (Table 2, run 11d). M_n of 10000 and 3000 g mol^{-1} were targeted for the EBR and PE segments, respectively. In this case, the polymerization was performed at 80°C and aliquots of the reaction medium were withdrawn before each switch of monomer feed. The evolution of the molar mass distribution after each step (initial EBR block, triblock, pentablock and heptablock formation) is given in Figure 1 and shows the excellent control over the successive chain extensions.

Table 2. Molar masses and thermal properties of PE-*b*-EBR-*b*-PE triblock and multiblock copolymers discussed in the manuscript.

Run	Polymer	Yield (g)	M_n theo [a] (g mol^{-1})	M_n SEC [b] (g mol^{-1})	$Đ$ [b]	T_g [c] (°C)	T_m [c] (°C)	T_c [c] (°C)	PE fraction (wt%)	Crystallinity of PE segments[d] (%)
9	PE_{3K}-*b*-EBR_{30K}-*b*-PE_{3K}	18.3	36600	38500	1.9	-32.1	114.1	91.9	17	60
10	PE_{6K}-*b*-EBR_{60K}-*b*-PE_{6K}	17.8	71200	71200	2.4	-32.0	119.2	99.5	17	59
11a	EBR_{10K}	-	10000	9400	1.7	-31.2	-	-	-	-
11b	PE_{3K}-*b*-EBR_{10K}-*b*-PE_{3K}	-	16000	16200	1.5	-29.6	113.9	100.6	38	42
11c	EBR_{10K}-*b*-PE_{3K}-*b*-EBR_{10K}-*b*-PE_{3K}-*b*-EBR_{10K}	-	36000	30700	1.8	-31.2	104.4	76.3	17	47
11d	PE_{3K}-*b*-EBR_{10K}-*b*-PE_{3K}-*b*-EBR_{10K}-*b*-PE_{3K}-*b*-EBR_{10K}-*b*-PE_{3K}	18.9	42000	41300	2.3	-30.8	101.8/121.3	100.4	29	46

Conditions: 200 mL of toluene, 4 bars, 90°C (80°C for run 11), E/B = 80/20 mol%, [Nd] = 250 µM, [MesMgBr] = 1.5 mM, [PDMB] = 2.5 mM (run 9 and 11), 1.25 mM (run 10) and [a] Mn^{theo} = yield/(nCTA), for the multiblock copolymer the expected M_n was considered. [b] Determined by SEC in 1,2,4-trichlorobenzene at 150°C. [c] Determined by DSC. [d] Determined by DSC $\Delta H_{100\%PE}$ = 293 J g^{-1}.

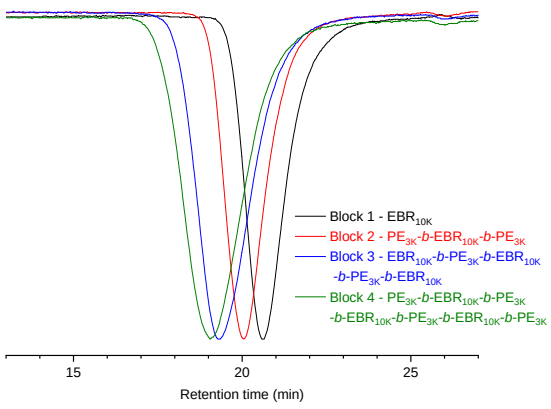

Figure 1. SEC chromatograms obtained after each switch of monomer feed during the synthesis of the heptablock copolymer.

Thermomechanical and rheological properties

DSC analysis (Table 1, Figures S5 and S6) of the diblock copolymers showed a T_g of EBR segments at about -33°C, a very weak meltng endotherm related to EBR segments around 10°C, and the melting of the PE block at 100-120°C. The normalized crystallinity of PE (See Table 1) is relatively low for short segments on low molar mass copolymers (15% and 33% for EBR_{15k}-*b*-PE_{3k} and EBR_{30k}-*b*-PE_{3k}, respectively) and the corresponding melting endotherms are very broad on DSC traces. In all other cases however, melting endotherms were narrow and the relative crystallinity was above 50%. Similar results were found for triblock copolymers PE-*b*-EBR-*b*-PE (Table 2, Figure S7), with the notable exception that even short PE_{3k} segments displayed high crystallinities of 60%.

Regarding the multiblock copolymer (Figure S8), the melting temperature of the PE block decreased when extending the PE-*b*-EBR-*b*-PE triblock (113.9°C) to the EBR-*b*-PE-*b*-EBR-*b*-PE-*b*-EBR pentablock (104.4°C) (Table 2). The heptablock displayed two distinct T_m that we attributed to internal (101.8°C) and external (121.3°C) PE blocks. Indeed, similar drastic changes in the crystallization temperature of internal or external blocks have already been observed in block copolymers based on poly(ε-caprolactone) and poly(trimethylene carbonate) segments.[25] Interestingly, the relative PE crystallinity barely changes in the three samples (See Table 2).

Extended thermomechanical information was obtained from DMA in tensile mode (Figure 2-a,b, Table S5) that enables to characterize the materials up to their melting point. Similar glass transition temperatures for all samples were confirmed. In the temperature range 0-30°C, the moduli appeared essentially driven by the fraction of PE, and reach at 25°C about 4 MPa for 9 wt% PE (run 4), about 11 MPa for 17 wt% PE (runs 2,5,9,10) and about 25 MPa for 29 wt% PE (runs 6 and 11d). Above 50°C, low molar mass diblocks EBR_{15k}-*b*-PE_{3k} and EBR_{30k}-*b*-PE_{3k}, and to a lower extent EBR_{30k}-*b*-PE_{6k}, softened progressively, thus confirming the broadness of the melting transition. The ratio $E'_{25°C}$ / $E'_{80°C}$ characterizes the conservation of properties in the service temperature range: triblock copolymers, even with short PE segments, performed significantly better than diblock copolymers. The multiblock copolymer, also containing short PE segments, demonstrated the least dissipative performance, with the lowest tan δ value at 80°C

While the two distinct melting transitions in the multiblock copolymer 11d can be clearly observed, analysis in tensile mode

is not adapted for melts, and to complete the monitoring of melting and crystallization we resorted to DMA experiments in a rheometer, using oscillatory shear by plate-plate geometries (Figure S9). The complex modulus G* during cooling-heating steps showed moderate hystereses between crystallization and melting, between 16 and 30°C, indicating fast crystallizations. In the melt, the complex moduli appeared to increase with the total molar mass of the copolymers, with however a surprisingly high value for EBR_{30k}-*b*-PE_{12k}. This was confirmed by small amplitude oscillatory shear (SAOS) at 150°C (Figure S10) that showed melts in or near terminal flow regime ($G'\sim\omega^2$, $G''\sim\omega^1$) except for EBR_{30k}-*b*-PE_{12k}. Finally, zero shear viscosities at 150°C were extrapolated from flow curves (Figure S11) and reported on Figure S12. While most samples obey the power law $\eta_0 \sim M^{3.4}$ characteristic of entangled melts, significant deviations are found for EBR_{15k} that appears to be below the critical entanglement molar mass, and for EBR_{30k}-*b*-PE_{12k} and EBR_{45k}-*b*-PE_{9k} that may present to a certain extent phase separation in the melt.

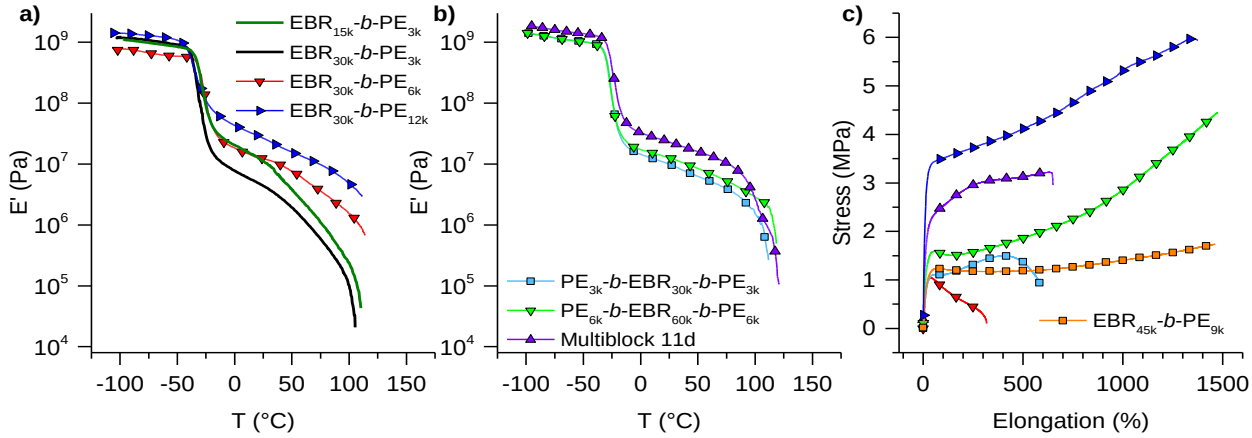

Figure 2. a,b) DMA analysis of block copolymers in tensile mode (1 Hz, 3°C min^{-1}). c) Tensile testing (RT, 500 mm min^{-1}). 1450% elongation corresponds to the maximal course and indicates that the samples did not break during the test.

Structural analysis

SAXS analyses at 150°C (Figure S13) confirmed that most EBR-*b*-PE block copolymers display featureless patterns, thus corroborating the absence of structuration in the melt. The good compatibility between the blocks could be indeed anticipated from the microstructure of EBR containing about 78 mol% of ethylene units (Table S2). In accordance with melt rheology, EBR_{45k}-*b*-PE_{9k} displayed however a broad scattering signal, rather distinctive of weak segregation without long range ordering. This could either stem from segregation between the PE and EBR blocks that may have reached a sufficient molar mass, or from the presence of a small amount of PE homopolymer that cannot be ruled out from SEC traces (Figure S2).

At room temperature (RT) however, sharp scattering peaks and corresponding 2*q** harmonics indicated strong microphase separation and formation of lamellar structures. Simultaneous SAXS/WAXS monitoring during cooling (see selected examples in Figure S14) indicated that this phase segregation is concomitant with crystallization of PE segments, and thus that these copolymers undergo crystallization-induced self-assembly from disordered melts. As a consequence, the morphology and interdomain spacings between crystalline PE lamellae are not necessarily dictated by the molar mass or the copolymers or the volume ratio of PE and EBR blocks.[26],[27] EBR_{15k}-*b*-PE_{3k} displayed for example longer interdomain spacing (58 nm) than EBR_{30k}-*b*-PE_{6k} (45 nm), most probably because of its lower crystallinity.

Direct imaging of the structuration was obtained by carefully surfacing bulk samples using ultracryo microtomy and imaging with PeakForce AFM. The same tip was kept for all images to allow for direct comparison of moduli between samples. The modulus images (Figure 3) show for all cases crystalline PE lamellae (in bright), separated with amorphous matrix. Profile analysis (see selected traces in Figure S15) shows interlamellar spacing in good accordance with the primary diffraction peak determined with SAXS. The moduli of crystalline lamellae measured with PeakForce (Figure S15) appears strongly correlated to the relative crystallinity within PE segments (Tables 1 and 2), varying typically between 20 MPa for weakly crystalline PE domains in EBR_{15k}-*b*-PE_{3k} to 200 MPa for highly crystalline PE domains in PE_{3k}-*b*-EBR_{30k}-*b*-PE_{3k}. Interestingly, the lamellae appeared also thicker and flatter for triblock copolymers than for the corresponding diblocks (Figure 3). In the multiblock copolymer 11d, no distinction can be made between two types of PE crystalline domains. The lamellae are however much smaller than in triblocks (no more than 200 nm large) and appear tightly packed.

Tensile properties

Tensile properties at RT of block copolymers displayed a variety of behaviors (Figure 2c, Table S5). Sample EBR_{15k}-*b*-PE_{3k} and EBR_{30k}-*b*-PE_{3k} had a viscoplastic behaviour that precluded conventional tensile testing. Initially, all materials displayed a rigid behaviour and a yield point at about 50% elongation typical of semicrystalline materials. The Young moduli *E* were in good accordance with DMA storage moduli at 25°C (See Table S5), and were essentially driven by the overall fraction of crystalline PE. This indicated to some extent a physical percolation between crystalline lamellae as confirmed by the AFM pictures showing intertwined lamellar stacks (Figure 3).

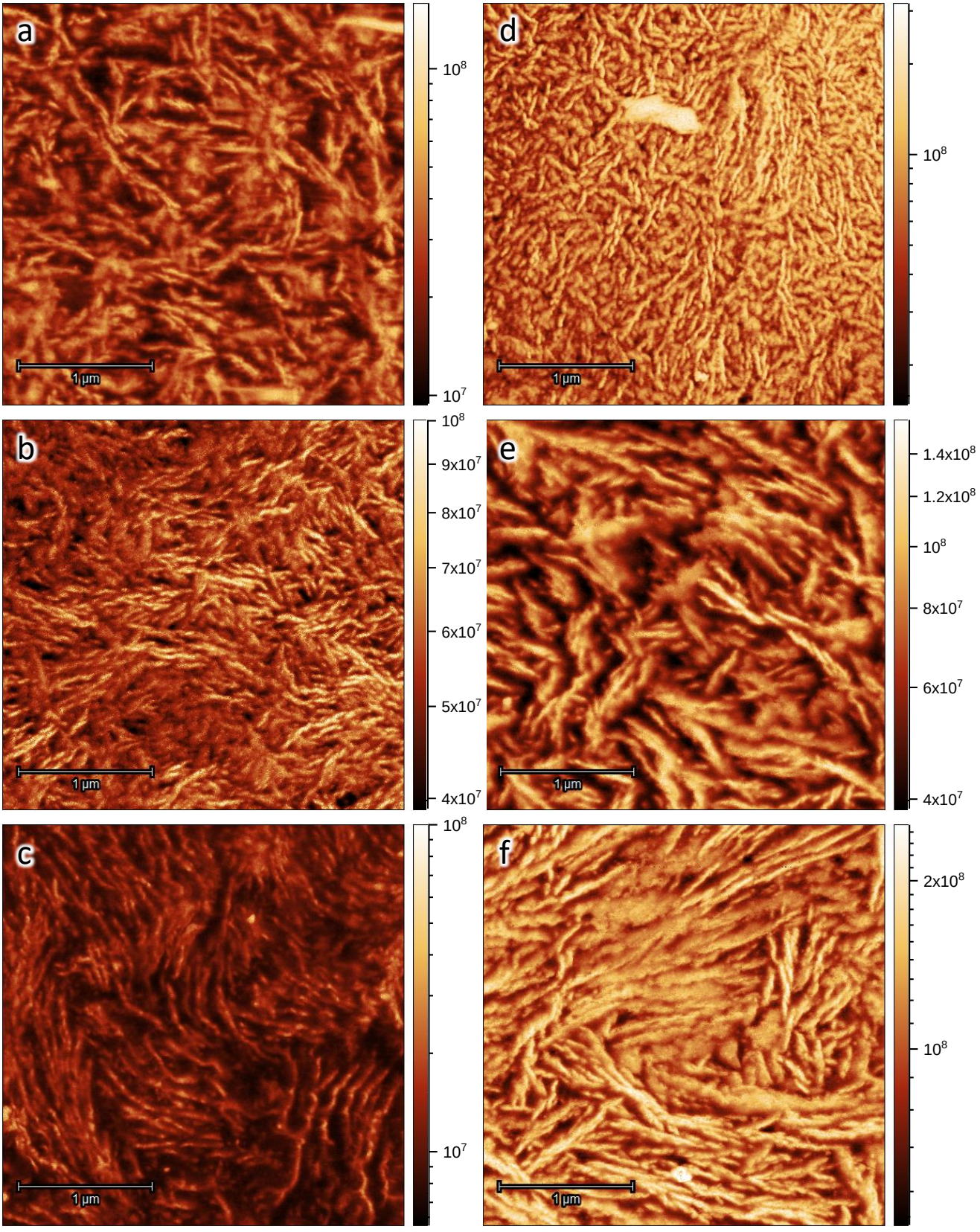

Figure 3. Modulus mapping through PeakForce AFM of samples a) EBR_{45k}-*b*-PE_{9k}, b) EBR_{30k}-*b*-PE_{6k}, c) EBR_{15k}-*b*-PE_{3k}, d) Multiblock 11d, e) PE_{6k}-*b*-EBR_{60k}-*b*-PE_{6k}, f) PE_{3k}-*b*-EBR_{30k}-*b*-PE_{3k}. The color scales are in Pa.

Elongation beyond the yield point eventually breaks apart physical interactions across lamellar stacks. The short EBR_{30k}-*b*-PE_{6k} diblock copolymer underwent ductile rupture while longer EBR_{30k}-*b*-PE_{12k} diblocks and EBR_{45k}-*b*-PE_{9k} deformed plastically up to the maximal course. In contrast, triblock and multiblock copolymers underwent strain hardening above 300% elongation demonstrating proper anchoring across crystalline lamellae. The triblock copolymer with short PE segments PE_{3k}-*b*-EBR_{30k}-*b*-PE_{3k} demonstrated limited strength (σ_{max}= 1.5 MPa), that we attributed to the relatively easy fragmentation or chain pullout from crystalline lamellae composed of low molar mass blocks. The multiblock 11d, also composed of short PE_{3k} segments showed in this regard improved strength (σ_{max} = 3.2 MPa) without compromises on the elongation at break, due to a higher fraction of crystalline materials. Finally, PE_{6k}-*b*-EBR_{60k}-*b*-PE_{6k} displayed far better strength with accelerated strain hardening occurring above 900% elongation similarly to chemically crosslinked elastomers and reached the maximal course of our tensile setup without breaking (σ_{max} > 4.4MPa, ε_b > 1450%).

The tensile characterization was completed by cyclic extensions to 300% to assess the elastic recovery (Figure S16 and Figure 4). This property is indeed critical for TPEs, that must be able to withstand repeated loads while maintaining their dimensional stability.

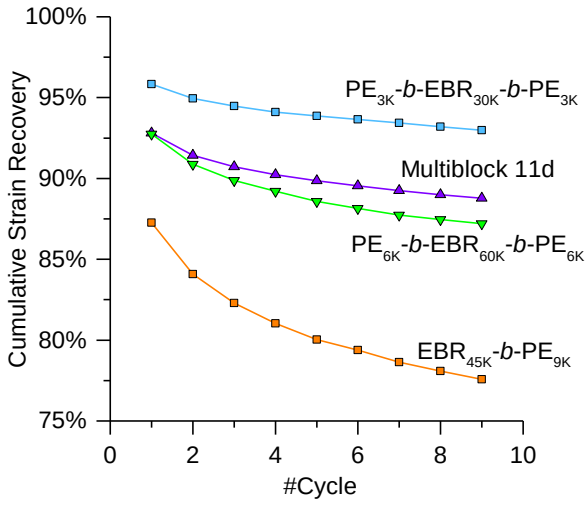

Figure 4. Elastic recovery after cyclic extension of the block copolymers at RT up to 300% elongation.

All block copolymers present a significant and irreversible loss of moduli and disappearance of yield behavior after the first stretching (Figure S16). As mentioned above, we attributed this to slip across lamellar stacks. The EBR_{45k}-*b*-PE_{9k} diblock copolymer performed relatively poorly as expected in absence of chain bridging across PE lamellae, and the corresponding strain recovery decayed continuously with each cycle. Triblock copolymers and especially the PE_{3k}-*b*-EBR_{30k}-*b*-PE_{3k} performed significantly better, with strain recoveries up to 93%. Finally, the multiblock 11d offered a very promising combination of high stiffness with excellent strain recovery up to 89%.

Conclusion

The development of polyolefin thermoplastic elastomers by catalytic routes is a major challenge for achieving recyclable polyolefin-based elastomers. We have shown in this paper that combining the control provided by CCTP and the design and use of original chain transfer agents such as bimetallic magnesium bromide allowed to synthesize from diblock to multiblock copolymers incorporating crystalline PE and elastomeric EBR segments in the same chain. Low molar mass copolymers (< 100 kg mol^{-1}) displaying low melt viscosities thanks to the absence of phase segregation in the melt underwent crystallization-driven self-assembly below 100°C. Depending on their macromolecular architectures (e.g. triblock or multiblock structures, segment molar mass and overall fraction of crystalline segments), a variety of mechanical properties can be achieved. The most promising material was PE_{6k}-*b*-EBR_{60k}-*b*-PE_{6k} triblock that demonstrate excellent extensibility above 1400% and strain recovery of 87% after 9 stretching cycles. In comparison, a multiblock ethylene-octene OBCs from Dow Chemical with a comparable content of 18 wt% in crystalline PE segments but a molar mass twice higher displayed similarly a low yield stress about 1.2 MPa, high extensibility up to 1200%, and an efficient elastic recovery of 94% after one cycle. Strain hardening at extensions > 500% is however much stronger due to a higher entanglement and leads to significantly higher ultimate tensile stress, at 14 MPa.[28] The PE_{3k}-*b*-EBR_{10k}-*b*-PE_{3k}-*b*-EBR_{10k}-*b*-PE_{3k}-*b*-EBR_{10k}-*b*-PE_{3k} multiblock copolymer also offered an excellent compromise with improved modulus, while also maintaining excellent strain recovery of 89% after 9 stretching cycles.

Acknowledgements

The authors thank the Manufacture Française des Pneumatiques Michelin for support and useful discussion. They thank the NMR Polymer Center of Institut de Chimie de Lyon (FR5223) for access to the NMR facilities and assistance. The authors acknowledge the Consortium Lyon Saint-Etienne de Microscopie (CLYM, FED 4092) for the access to the AFM microscope. The AFM characterization was supported by the LABEX iMUST of the University of Lyon (ANR-10-LABX-0064), created within the "Plan France 2030" set up by the french government and managed by the French National Research Agency (ANR). Julie Bratasanu is acknowledged for the preparation of AFM samples. We acknowledge the European Synchrotron Radiation Facility (ESRF) and SOLEIL for provision of synchrotron radiation facilities and we would like to thank Isabelle Morfin and Thomas Bisien for support in using beamlines BM02@ESRF and

SWING@Soleil, respectively, as well as Fabrice Brunel for performing temperature-dependent SAXS/WAXS experiments.

Data Availability Statement

The data that support the findings of this study are available in the Supporting Information of this article.

Keywords: polyolefin • thermoplastic elastomers • block copolymer • ethylene • butadiene

References

[1] W. Wang, W. Lu, A. Goodwin, H. Wang, P. Yin, N.-G. Kang, K. Hong, J. W. Mays, *Prog. Polym. Sci.* **2019**, *95*, 1–31.
[2] G. Holden, N. R. Legge, R. P. Quirk, H. E. Schroeder, Eds. , *Thermoplastic Elastomers*, Hanser, Munich, **1996**.
[3] T. Stößer, D. Mulryan, C. K. Williams, *Angew. Chem. Int. Ed.* **2018**, *57*, 16893–16897.
[4] A. C. Deacy, G. L. Gregory, G. S. Sulley, T. T. D. Chen, C. K. Williams, *J. Am. Chem. Soc.* **2021**, *143*, 10021–10040.
[5] J. Meimoun, C. Sutapin, G. Stoclet, A. Favrelle, P. Roussel, M. Bria, S. Chirachanchai, F. Bonnet, P. Zinck, *J. Am. Chem. Soc.* **2021**, *143*, 21206–21210.
[6] G. Zanchin, G. Leone, *Prog. Polym. Sci.* **2021**, *113*, 101342.
[7] G. J. Domski, J. M. Rose, G. W. Coates, A. D. Bolig, M. Brookhart, *Prog. Polym. Sci.* **2007**, *32*, 30–92.
[8] V. C. Gibson, *Science* **2006**, *312*, 703–704.
[9] R. Kempe, *Chem. – Eur. J.* **2007**, *13*, 2764–2773.
[10] L. R. Sita, *Angew. Chem. Int. Ed.* **2009**, *48*, 2464–2472.
[11] F. D'Agosto, C. Boisson, *Aust. J. Chem.* **2010**, *63*, 1155–1158.
[12] A. Valente, A. Mortreux, M. Visseaux, P. Zinck, *Chem. Rev.* **2013**, *113*, 3836–3857.
[13] D. J. Arriola, E. M. Carnahan, P. D. Hustad, R. L. Kuhlman, T. T. Wenzel, *Science* **2006**, *312*, 714–719.
[14] P. D. Hustad, R. L. Kuhlman, D. J. Arriola, E. M. Carnahan, T. T. Wenzel, *Macromolecules* **2007**, *40*, 7061–7064.
[15] S. D. Kim, T. J. Kim, S. J. Kwon, T. H. Kim, J. W. Baek, H. S. Park, H. J. Lee, B. Y. Lee, *Macromolecules* **2018**, *51*, 4821–4828.
[16] S. S. Park, C. S. Kim, S. D. Kim, S. J. Kwon, H. M. Lee, T. H. Kim, J. Y. Jeon, B. Y. Lee, *Macromolecules* **2017**, *50*, 6606–6616.
[17] V. Monteil, R. Spitz, F. Barbotin, C. Boisson, *Macromol. Chem. Phys.* **2004**, *205*, 737–742.
[18] J. Thuilliez, L. Ricard, F. Nief, F. Boisson, C. Boisson, *Macromolecules* **2009**, *42*, 3774–3779.
[19] I. Belaid, B. Macqueron, M.-N. Poradowski, S. Bouaouli, J. Thuilliez, F. D. Cruz-Boisson, V. Monteil, F. D'Agosto, L. Perrin, C. Boisson, *ACS Catal.* **2019**, *9*, 9298–9309.
[20] N. Baulu, M. Langlais, R. Ngo, J. Thuilliez, F. Jean-Baptiste-dit-Dominique, F. D'Agosto, C. Boisson, *Angew. Chem. Int. Ed.* **2022**, *61*, e202204249.
[21] N. Baulu, M. Langlais, P. Dugas, J. Thuilliez, F. Jean-Baptiste-dit-Dominique, M. Lansalot, C. Boisson, F. D'Agosto, *Chem. – Eur. J.* **2022**, *28*, e202202089.
[22] H. E. Park, J. M. Dealy, G. R. Marchand, J. Wang, S. Li, R. A. Register, *Macromolecules* **2010**, *43*, 6789–6799.
[23] C. De Rosa, R. Di Girolamo, A. Malafronte, M. Scoti, G. Talarico, F. Auriemma, O. Ruiz De Ballesteros, *Polymer* **2020**, *196*, 122423.
[24] N. Baulu, M.-N. Poradowski, L. Verrieux, J. Thuilliez, F. Jean-Baptiste-dit-Dominique, L. Perrin, F. D'Agosto, C. Boisson, *Polym. Chem.* **2022**, *13*, 1970–1977.
[25] R. V. Castillo, G. Fleury, C. Navarro, A. Couffin, D. Bourissou, B. Martín-Vaca, *Eur. Polym. J.* **2017**, *95*, 711–727.
[26] A. J. Müller, V. Balsamo, M. L. Arnal, in *Block Copolym. II* (Ed.: V. Abetz), Springer-Verlag, Berlin/Heidelberg, **2005**, pp. 1–63.
[27] R. M. Van Horn, M. R. Steffen, D. O'Connor, *Polym. Cryst.* **2018**, *1*, DOI 10.1002/pcr2.10039.
[28] H. P. Wang, D. U. Khariwala, W. Cheung, S. P. Chum, A. Hiltner, E. Baer, *Macromolecules* **2007**, *40*, 2852–2862.